Physical Chemistry Chemical Physics

PCCP

Interaction of cisplatin and two potential antitumoral platinum(II) complexes with a model lipid membrane: a combined NMR and MD study

Journal:	*Physical Chemistry Chemical Physics*
Manuscript ID:	CP-ART-09-2014-004360.R1
Article Type:	Paper
Date Submitted by the Author:	07-Nov-2014

Complete List of Authors:	Nierzwicki, Lukasz; Gdansk University of Technology, Department of Physical Chemistry Wieczor, Milosz; Gdansk University of Technology, Department of Physical Chemistry Censi, Valentina; University of Pisa, Department of Chemistry and Industrial Chemistry; Politecnico di Bari, Department DICATECh Baginski, Maciej; Gdansk University of Technology, Department of Pharmaceutical Technology and Biochemistry Calucci, Lucia; Consiglio Nazionale delle Ricerche, Istituto di Chimica dei Composti OrganoMetallici Samaritani, Simona; University of Pisa, Department of Chemistry and Industrial Chemistry Czub, Jacek; Gdansk University of Technology, Department of Physical Chemistry Forte, Claudia; CNR, Istituto di Chimica dei Composti Organometallici

PCCP

RSCPublishing

ARTICLE

Interaction of cisplatin and two potential antitumoral platinum(II) complexes with a model lipid membrane: a combined NMR and MD study

Cite this: DOI: 10.1039/xoxxoooooox

Received
Accepted

DOI: 10.1039/xoxxoooooox

www.rsc.org/

L. Nierzwicki,[a] M. Wieczor,[a] V. Censi,[b‡] M. Baginski,[c] L. Calucci,[d] S. Samaritani,[b] J. Czub[a]† and C. Forte[d]†

In this study, the interaction of cisplatin (**1**) and two potential antitumoral Pt(II) complexes (**2** and **3**) with a model DMPC bilayer was investigated by multinuclear NMR spectroscopy and MD simulations in order to understand its implication on the different antitumoral properties shown by the three complexes. In particular, ^{31}P, ^{13}C and ^{2}H solid state NMR experiments were performed to obtain information on the phase structure, phase transitions and structural and dynamic changes in the phospholipid bilayer upon interaction with the platinum complexes. On the other hand, MD calculations yielded free energy profiles for the different complexes across the bilayer; the results were analysed to obtain MD predictions on complex distribution with respect to the bilayer, as well as to establish their effects on the conformational equilibrium of the DMPC acyl chains. The combination of NMR and MD approaches highlighted that, whereas the more hydrophilic cisplatin tends to remain in the polar head group region, causing a decrease in flexibility of the bilayer, the two new complexes enter into the bilayer. In particular, complex **2** is preferentially located relatively close to the surface, only slightly affecting the bilayer structure and mobility, while complex **3** penetrates more deeply, strongly perturbing the bilayer and giving rise to lateral phase separation.

Introduction

Platinum complexes, as cisplatin (**1** in Fig. 1), oxaliplatin and carboplatin, are potent antitumor drugs widely used in chemotherapy.[1] Notwithstanding their severe dose-limiting side effects and loss of efficiency during therapy due to tumor resistance that may be acquired, the effective antitumoral activity of platinum compounds is well recognized, and consequently great effort is dedicated to the design of new platinum(II)-based drugs and to the development of improved delivery strategies to tumors.[2,3]

One of the issues that must be dealt with when designing new drug candidates is their capacity to overcome biological membrane barriers. Traditionally, the method by which Pt drugs enter cells has been attributed to simple passive diffusion, although it is by now recognized that cisplatin enters cells also through carrier-mediated transport.[4,5] In the transmembrane diffusion process the size and hydrophilic nature of drugs play a significant role. Hence, it is not surprising that in recent research on new Pt(II)-based drug design attention is devoted to the choice of ligands with suitable properties which may regulate passive diffusion, as for example polarity, hydrophilicity, and steric hindrance.

Recently, Pt(II) complexes containing a triphenylphosphine ligand were synthesized by some of us, and their antiproliferative activity on three human tumor cell lines was evaluated.[6] It was found that the trans-[dichloro{N,N-bis(2-hydroxyethyl) amino} (triphenylphosphino) platinum(II)] complex (**2** in Fig. 1) has a cytotoxic effect comparable to that of cisplatin on HeLa (cervix adenocarcinoma), A549 (non-small cell lung cancer) and H460 (large cell lung cancer) cell lines. It is worthy of note that this complex is a trans Pt(II) complex and only recently it has been ascertained that this type of complexes may be endowed with antitumor activity, similarly to the cis Pt(II) ones.[7] On the other hand, the cis-[dichloro(carbonyl) (triphenylphosphino)platinum(II)] complex[8] (**3**, see Fig. 1) was found to have negligible antiproliferative effects against the same cell lines.[9]

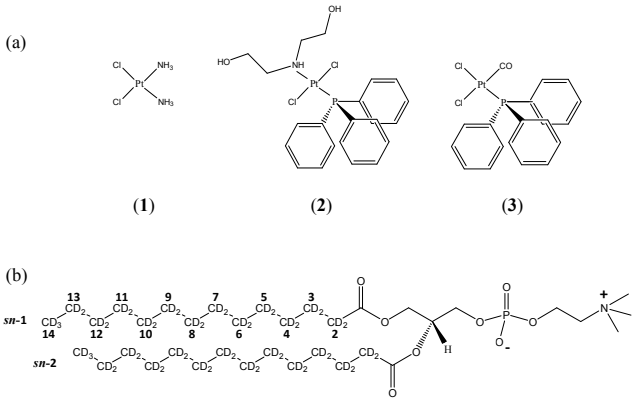

Figure 1. (a) Platinum(II) complexes studied in this work. (b) DMPC-d_{54} structure with carbon position numbering.

The different antiproliferative activity observed *in vitro* for complexes **2** and **3**, also compared to cisplatin (**1**) (see GI_{50}

values in Table S1 in the Supporting Information), prompted us to investigate their interaction with the cell membrane, drug-membrane interactions playing an important role in drug transport, distribution, accumulation, efficacy, and resistance. To this end, the 1,2-dimyristoyl-sn-glycero-3-phosphocholine (DMPC) phospolipid bilayer was chosen as a model membrane since phosphatidylcholines represent the most abundant lipid class in mammalian plasma membranes. Furthermore, DMPC has the advantage of being in the physiologically relevant liquid crystalline L_α phase at room temperature when hydrated with at least 20 wt% of water.[10]

The Pt complexes-membrane interactions, which usually are manifested by changes in the physical and thermodynamic properties of the membranes, were investigated by combining nuclear magnetic resonance (NMR) spectroscopy and molecular dynamics (MD) calculations. The two methods, although covering different motional time scales (in the micro- to milliseconds range the former, in the nano- to microseconds range the latter), provide largely complementary views of membrane molecular structure, orientational order, and dynamics. NMR spectroscopy is recognized as a useful technique for studying drug-membrane interactions since, thanks to the possibility of exploiting different nuclei (as ^{31}P, ^{13}C and ^{2}H) and of applying different experiments, it allows structural and dynamic information on the different regions of the phospholipid bilayer to be selectively obtained, in addition to giving information on the phase structure and phase transitions.[11,12] On the other hand, MD simulations provide direct insight into structural and dynamic parameters of phospholipid bilayers[13] and thus allow the effects of membrane-interacting molecules, such as drugs, on the bilayer properties to be studied with atomic resolution. Distribution of drug molecules across the bilayer, the bilayer/water partitioning, and permeability properties can also be predicted fairly well.[14,15]

In this study, ^{2}H, ^{31}P and ^{13}C solid state NMR techniques and MD calculations were applied on DMPC multilamellar vesicles (MLVs) doped with cisplatin, complex **2,** and complex **3**. MLVs were prepared using 32 wt% of water, that is an amount that guarantees the formation of relatively large bilayers avoiding a large pool of bulk water; in these conditions drug-bilayer interactions are expected to be enhanced. The NMR and MD findings were combined allowing the interactions of the different complexes with the DMPC bilayer to be examined in a biologically relevant manner obtaining a consistent and detailed picture of the distribution of the complexes within the model membrane.

Results

^{31}P NMR spectra

The ^{31}P NMR spectra of all the investigated samples, reported in Figure 2, showed the typical powder pattern observed for non-uniformly aligned phospholipid bilayers and arising from axially symmetric motional averaging of the ^{31}P chemical shift tensor due to rapid motion of the molecules around an axis perpendicular to the bilayer surface or rapid intramolecular isomerization of the head group.[16,17] Consequently, the lineshapes are characterized by two discontinuities, corresponding to the time-averaged chemical shift tensor components $\sigma_\perp$ and $\sigma_\parallel$, from which the effective chemical shift anisotropy $\Delta\sigma$ ($= \sigma_\parallel - \sigma_\perp$) can be determined.

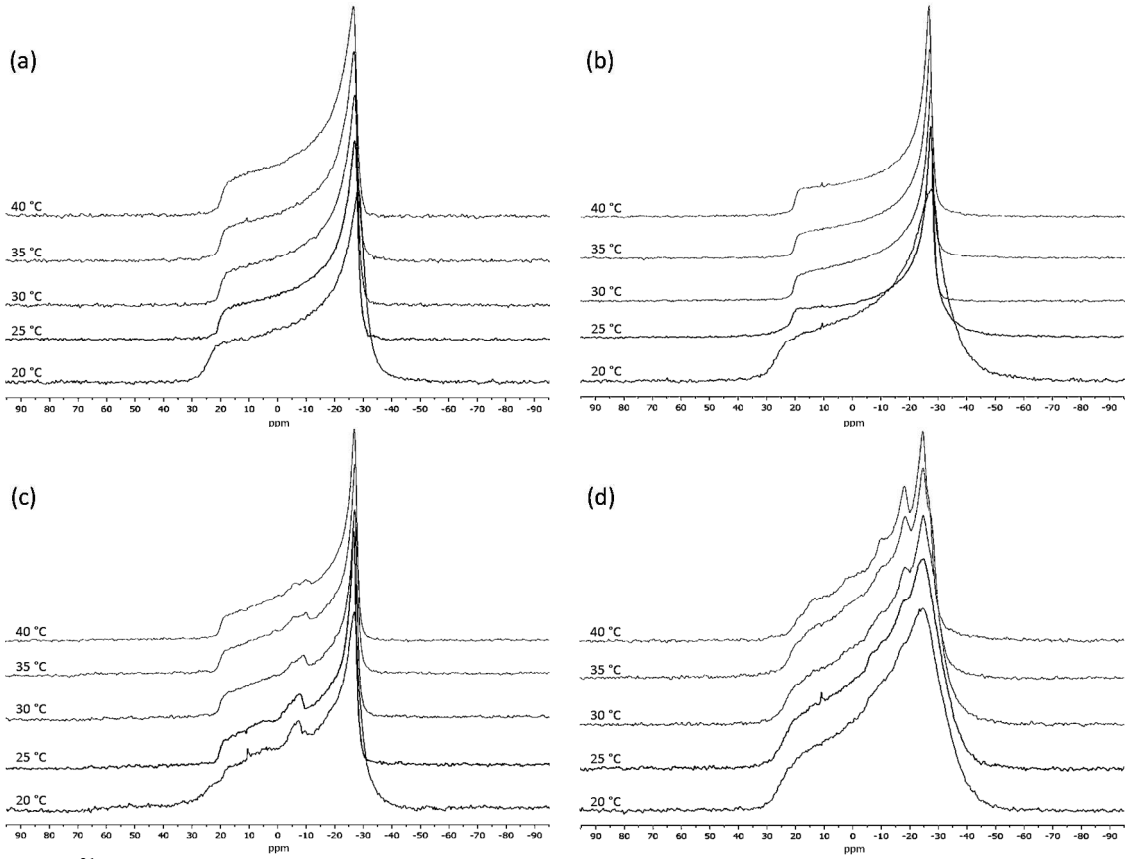

Figure 2. ^{31}P NMR spectra at different temperatures of (a) **DMPC**, (b) **DMPC/1**, (c) **DMPC/2**, and (d) **DMPC/3**.

PCCP RSCPublishing

ARTICLE

The spectra of **DMPC** and **DMPC/1**, which were quite similar at each temperature, showed an abrupt decrease in Δσ upon heating from 20 to 25 °C due to the gel to the liquid crystalline L_α phase transition and only minor changes between 25 °C and 40 °C (Figure 2a and 2b). A similar behaviour was observed for the spectra of **DMPC/2** (Figure 2c), the only difference lying in the presence of an additional signal ascribed to the triphenylphosphine ligand on the basis of the ^{31}P magic angle spinning (MAS) NMR spectrum (not shown). In the case of **DMPC/3** (Figure 2d), the spectra at lower temperatures were quite broadened reflecting a relatively disordered $P_{\beta'}$ phase at 20 °C and at least two different phospholipid environments above 20 °C, more clearly visible at higher temperatures, in addition to a signal arising from the triphenylphosphine ligand. In none of the samples there was evidence of an isotropic or an hexagonal phase.[17]

Table 1. Chemical shift anisotropy values determined from the fitting of ^{31}P NMR spectra.

Sample	Δσ (ppm)[a]				
	20 °C	**25 °C**	**30 °C**	**35 °C**	**40 °C**
DMPC	54	49	48	48	47
DMPC/1	57	50	49	48	47
DMPC/2	53	48	48	48	47
DMPC/3	-	-			49 (η=0.12) 33

[a] maximum error is 1 ppm.

The application of a fitting procedure allowed Δσ to be determined for the different samples at all temperatures, except for **DMPC/3**; in this case, the fitting procedure could be successfully applied only at the highest temperature (40 °C) where the spectrum was better resolved. In this case two spin systems were required for a good fitting (see Figure S1 in the Supporting Information). The Δσ values obtained for the different samples are reported in Table 1. The data showed a significantly higher Δσ value for **DMPC/1** with respect to **DMPC** at 20°C, the difference decreasing with increasing temperature and disappearing at 35 °C. On the contrary, no significant differences were found between **DMPC/2** and **DMPC** at all the investigated temperatures. In the case of **DMPC/3**, one component had axial symmetry but a significantly smaller Δσ value with respect to those observed for the other samples at the same temperature, whereas the other had a non-zero asymmetry parameter (η) and a slighlty higher Δσ value.

^{2}H NMR spectra

The ^{2}H NMR spectra of all the investigated samples, containing DMPC-d_{54} fully deuterated on the acyl chains, are shown in Figure 3. The ^{2}H NMR spectra of **DMPC**, similar to those already reported in the literature for DMPC MLVs,[18,19] were indicative of a spherical distribution of the axes perpendicular to the bilayers, with no preferential orientation of the bilayers with respect to the external magnetic field. Moreover, the spectra were characteristic of axially symmetric motions of the phospholipids about the bilayer normal, with a distribution of quadrupolar splittings due to the various inequivalent methylene and methyl groups of the perdeuterated acyl chains. In particular, at all temperatures, the **DMPC** sample showed the typical lineshape observed for an L_α phase with a width that decreased with increasing temperature (Figure 3a), in agreement with an expected $P_{\beta'}$- L_α transition temperature (T_c) < 20 °C for DMPC-d_{54}.[20] Differently from **DMPC**, at the low temperatures, samples **DMPC/1** and **DMPC/2** (Figure 3b and 3c, respectively) showed the typical powder lineshape of the gel phase. At the higher temperatures, the only difference observed among **DMPC**, **DMPC/1** and **DMPC/2** lay in the overall spectral width, this being largest for the sample containing cisplatin and smallest for the undoped sample, also taking into account the different T_c. To this regard, it is to be noted that the presence of complex **1** causes an increase in T_c also with respect to complex **2**. However, in the following, no corrections were attempted for the differences in T_c due to the different content of DMPC-d_{54} in the samples, since this does not affect the qualitative considerations that will be made. A quite different behaviour was observed for **DMPC/3** (Figure 3d). In this case, the ^{2}H spectra clearly resulted from a superposition of powder spectra characterized by a significant difference in order and mobility, which changed with temperature. In particular, a subspectrum ascribable to the gel phase was present at least up to 30 °C, its contribution decreasing on heating. On the other hand, a subspectrum with features characteristic of the L_α phase was already present at 20 °C, as indicated by the sharp methyl doublet, becoming clearly evident at 40 °C, and its relative contribution increasing upon heating. At 30 °C, another subspectrum emerged, having features surprisingly very similar to those observed in ^{2}H NMR spectra of liquid-ordered (L_o) phases which form, for example, in ternary phospholipids and cholesterol mixtures.[21] The ^{2}H NMR spectra in the L_o phase are similar to those in the L_α one but with much higher spread in frequency and two distinct signals for the methyl deuterons of the two DMPC chains, as clearly observed here in the spectra recorded at 35 and 40 °C.
Except for sample **DMPC/3**, the quadrupolar splittings ($\Delta\nu_{q,i}$) for each distinguishable quadrupolar doublet, corresponding to different methylene and methyl groups of the acyl chains, were determined at different temperatures within the L_α phase, exploiting the better resolution obtained from the de-Paked spectra,[22] an example of which is shown in Figure S2 (Supporting Information). The assignment of the different doublets was made on the basis of literature data for selectively deuterated[23-26] and perdeuterated[19,27] DMPC, which indicate

that similar splittings for the two acyl chains can be reasonably assumed from the second methylene group of the chains (numbered 3 in Fig.1) onwards. As far as the first methylene group is concerned, experiments on selectively deuterated DMPC have shown significant differences both between the *sn*-1 and *sn*-2 chains, the latter having quite smaller quadrupolar splittings, and between the two deuterons of the *sn*-2 methylene group which are not magnetically equivalent.[23-25] This considered, in the following the data for the *sn*-1 chain are taken into account, and the assignment made by Petrache et al.[19] was used.

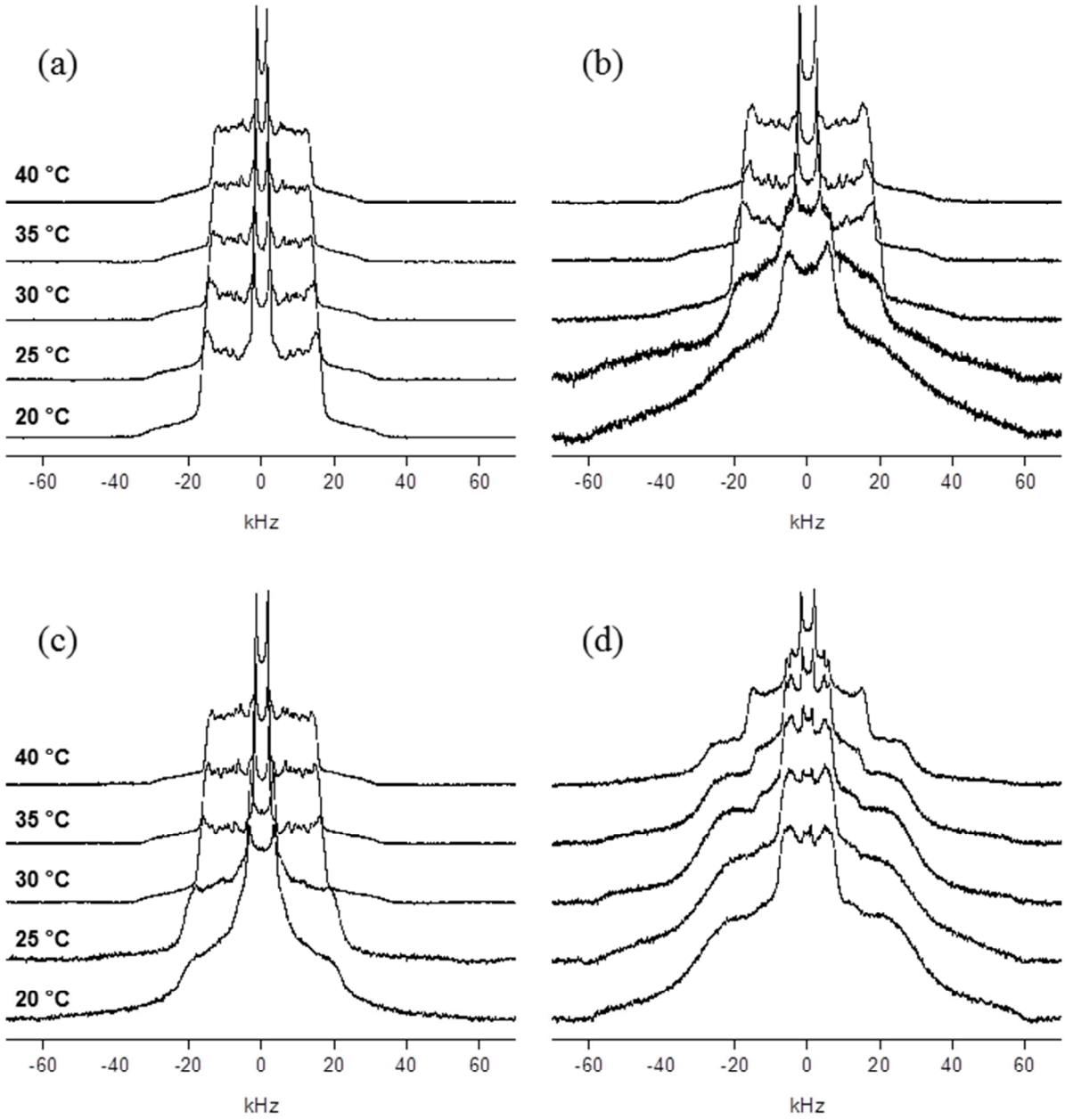

Figure 3. ^{2}H NMR spectra of (a) **DMPC**, (b) **DMPC/1**, (c) **DMPC/2**, and (d) **DMPC/3**.

The Pt(II) complexes **1** and **2**, although affecting the $\Delta\nu_{q,i}$ values, did not change the overall shape of the spectra above T_c, and, hence, the doublets were assigned with the reasonable assumption that their relative position in the spectrum was not changed. This assumption was confirmed by the order parameters determined from MD calculations (*vide infra*). The spectral assignment and the corresponding quadrupolar splittings ($\Delta\nu_{q,i}$) for **DMPC**, **DMPC/1** and **DMPC/2** at 35 °C are reported in Table S2 (Supporting Information). The measured $\Delta\nu_{q,i}$ values were used to determine the local order parameters S_{CDi} according to equation:[11]

$$\Delta\nu_{q,i} = \frac{3}{2} q S_{CD_i} \left(\frac{3cos^2\theta - 1}{2}\right) \quad (1)$$

with q the quadrupolar coupling constant (taken equal to 167 kHz)[28] and θ the angle between the bilayer normal and the

magnetic field. In de-Paked spectra, which correspond to an aligned sample with the bilayer normal parallel to the external magnetic field, θ is equal to 0°. The S_{CDi} are related to the average orientation of the *i*-th C-D bond with respect to the director of the phase, thus providing a quantitative measure of the degree of order along the lipid acyl chains. Generally, they can assume values from –0.5 to 1, however in phospholipid bilayers with the director along the external magnetic field, they are typically negative ranging between -0.5, in the case of a perfectly ordered acyl chain in all-trans conformation and rapidly rotating about the bilayer normal, and 0 in the case of an isotropically averaged system. This given, in the following the absolute values will be reported for simplicity of graphical representation. The S_{CD} absolute values determined for the *sn*-1 acyl chain for **DMPC**, **DMPC/1** and **DMPC/2** at 35 and 40 °C are plotted as a function of carbon position in Figure 4a. The magnitude of the local order parameters indicated that the lipid chains possessed considerable disorder due to trans-gauche rotation isomerizations, in addition to whole molecule rotations and wobbling motions. The acyl segments close to the glycerol backbone, i.e. at the beginning of the acyl chains, all possessed a similar degree of disorder, with relatively constant S_{CD} values; further on along the chain, the order parameters steadily decreased going towards the chain end. Furthermore, with increasing temperature, the order parameters decreased reflecting the expected increase in chain disorder.

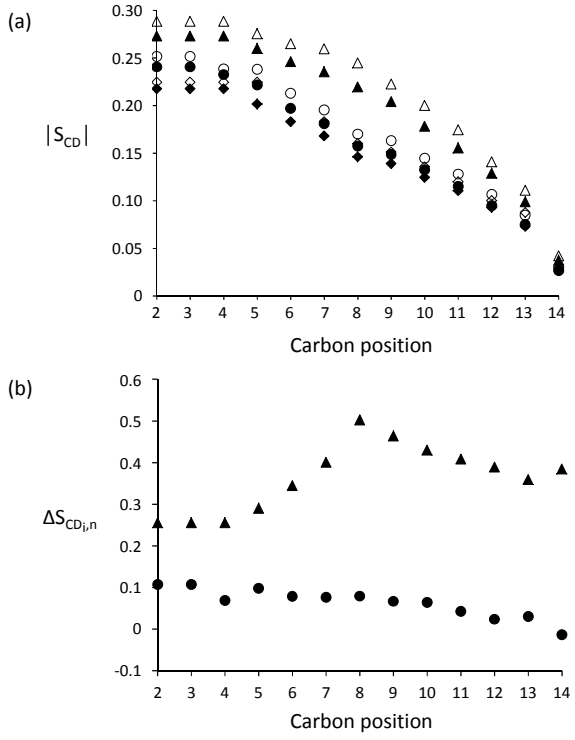

Figure 4. (a) Absolute S_{CD} values for the different deuterated positions along the DMPC *sn*-1 acyl chain at 35 °C (closed symbols) and 40 °C (open symbols) for: (◆ and ◇) **DMPC**, (▲ and △) **DMPC/1**, and (● and ○) **DMPC/2**. (b) Normalized S_{CD} changes for the different deuterated positions along the acyl chains at 35 °C for: (▲) **DMPC/1**, and (●) **DMPC/2**.

As evidenced in Figure 4a, the presence of complex **1** induced a significant ordering of the phospholipid alkyl chains, whereas complex **2** caused only a minor ordering effect. However the ordering effect in the case of complex **1** was not uniform along the chain. In order to put this effect in evidence, it is useful to consider the normalized relative change in order parameter along the chain upon addition of the complex ($\Delta S_{CD_{i,n}}$) which can be evaluated using the following equation:[29]

$$\Delta S_{CD_i,n} = \frac{S_{CD_i}(\text{lipid+complex}) - S_{CD_i}(\text{lipid})}{S_{CD_i}(\text{lipid})}. \quad (2)$$

The $\Delta S_{CD_{i,n}}$ values are reported in Figure 4b for **DMPC/1** and **DMPC/2** at 35 °C. For complex **1**, an increase in order was observed for all methylene groups, which was higher for the central region of the chains, i.e. from methylene 6 to 9. On the other hand, for complex **2** a small ordering effect was found, higher for the first few methylene groups and uniformly decreasing along the chain to vanish after the 11th methylene position.

Two bilayer structural parameters which are strongly related to the degree of chain ordering, i.e. the bilayer thickness (*d*) and the surface area per lipid molecule (*A*), were determined from the acyl chain order parameters following the procedure described in the Supporting Information. The *d* and *A* values found for **DMPC** (21.7 Å and 61.0 Å^2, respectively) were similar to those reported in the literature.[30] As expected, the data clearly showed that, in the presence of complex **1,** the bilayer thickness was significantly larger (*d* = 23.6 Å) and, correspondingly, the area per lipid molecule was quite smaller (*A* = 55.9 Å^2). Complex **2** induced similar but significantly smaller effects being *d* = 22.1 Å and *A* = 59.4 Å^2.

^{13}C CP-MAS NMR spectra

The ^{13}C CP-MAS spectra of DMPC can be divided into three chemical shift ranges: between 10 and 40 ppm resonate the carbons in the hydrophobic region, between 40 and 80 ppm those in the glycerol backbone and head group regions, and near 170 ppm the esterified carbonyls.[31] The ^{13}C NMR spectra recorded on **DMPC/1** and **DMPC/2** were identical to those reported in the literature for DMPC. For these samples, upon heating from 20 °C, the only changes observed were in the acyl chain methylene carbons signals, and particularly the more intense signal at ~31 ppm due to methylene carbons from 4 to 11, which showed a consistent but gradual upfield shift, from 31.5 to 30.8 ppm, due to the onset, above T_c, of trans-gauche isomerization in the chain, the gauche conformation in methylene chains being characterized by a smaller ^{13}C chemical shift value with respect to the trans conformation.[32] The 20-40 ppm region of the spectra of **DMPC/1** recorded at the different

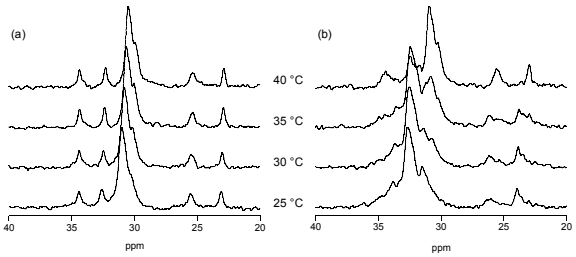

Figure 5. ^{13}C CP-MAS NMR spectra (20-40 ppm region) at different temperatures of (a) **DMPC/1** and (b) **DMPC/3**.

temperatures are shown in Figure 5 together with those obtained for DMPC/3. In the case of the latter sample, differently from **DMPC/1** and **DMPC/2**, the signals were broader, symptom of either conformational heterogeneity or lower mobility. Furthermore, at 20 °C the most intense C4-C11 signal had a chemical shift value at 32.7 ppm, hence more than 1 ppm higher than that observed for the other samples; with increasing the temperature, this signal remained at the same chemical shift value but its intensity decreased and, correspondingly, a new signal emerged at the chemical shift of the signal observed for the other samples at the higher temperatures (30.8 ppm at 40 °C).

MD simulations

The free energy profiles computed for the three complexes are shown in Figure 6a (for the convergence plots see Figure S3). For the quite polar complex **1**, the bilayer presented a pronounced (12 kcal/mol) energy barrier, rendering the transmembrane diffusion process inefficient. Complex **1** was only slightly less likely to reside in the polar headgroup region than in the water phase. The opposite was found for the hydrophobic complexes **2** and **3**, which tended to accumulate within the bilayer, as revealed by a broad free energy well associated with the hydrocarbon region. Notably, in the case of complex **2** this free energy well was deeper (6-7 kcal/mol) and the barrier at the bilayer midplane was visibly higher (5 kcal/mol) than for complex **3** (with values of 4-6 and 2 kcal/mol, respectively). It is worth noting that the employed model neglects the polarizability of both the platinum complexes and the lipid bilayer. This assumption may affect the obtained free energy profiles, also considering that membrane permeation involves a major change in the dielectric properties of the environment and that the platinum (II) ion is highly polarizable. However, the behavior of the complexes here examined is mostly determined by steric properties, which remain unaffected by such environmental changes.[33,34]

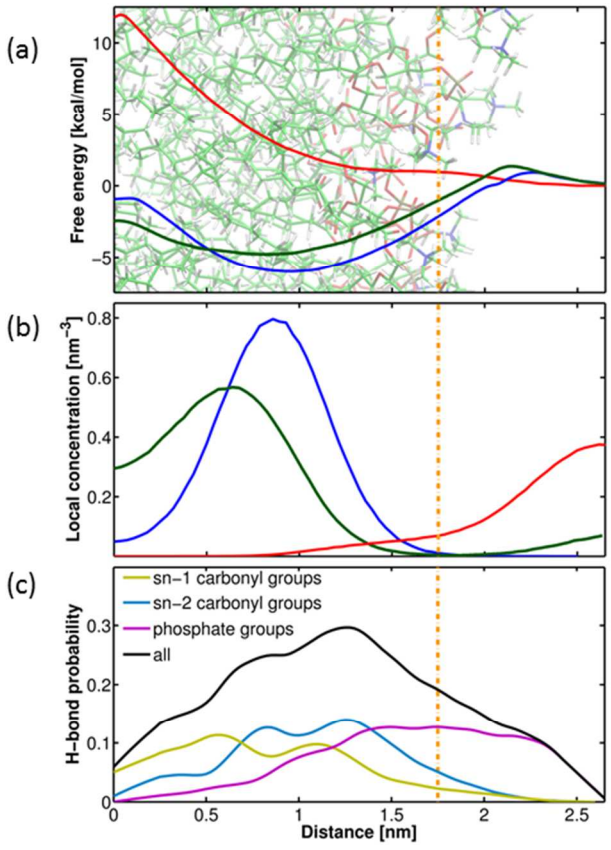

Figure 6. Trends as a function of the distance between the platinum atom and the bilayer midplane of: (a) free energy for the transfer of complex **1** (red), complex **2** (blue) and complex **3** (green) across one leaflet of the DMPC bilayer; (b) concentration of complex **1** (red), complex **2** (blue) and complex **3** (green) molecules; (c) probability of hydrogen bond formation between complex **2** and the carbonyl and phosphate groups of DMPC. Vertical orange line: average distance of the DMPC phosphate groups from the bilayer midplane.

Two different partition coefficients (logP) were calculated, one corresponding to the water/bilayer partitioning (see Supporting Information) and the other describing the partitioning between the polar part of the system (which includes water and the DMPC polar head groups) and the hydrocarbon chain region. Since biochemical partition coefficients are typically measured for the water/n-octanol system, the latter parameter is presumably more experimentally relevant. For comparison, the partition coefficients were also predicted based on the Pt complexes' structure using the online utility Molinspiration.[35] The results are summarized in Table 2 together with the experimental value reported in the literature for cisplatin.[36] It can be seen that the logP value calculated for cisplatin considering the partitioning between the polar and hydrophobic regions fitted the experimental one much better than that obtained considering the bilayer and water regions, as well as that calculated on the basis of molecular structure. Another noteworthy result is that logP values obtained for complexes **2** and **3**, contrarily to complex **1**, are positive and lie in the 1-4 range, i.e. the range where logP values of most traded drugs showing relatively easy membrane penetration fall. The differences in the membrane penetration between the studied complexes suggested by the logP values are further confirmed by the membrane permeability coefficients *p* which were found equal to 6.67×10^{-7}, 4.17×10^{-4} and 8.02×10^{-4} cm·s^{-1} for complexes **1**, **2** and **3**, respectively, determined as described in the Supporting Information.

In order to understand the reasons underlying the highest affinity to the membrane found for complex **2**, the probability of hydrogen bond formation between this complex and DMPC headgroups was calculated (see Experimental). As can be seen in Figure 6c, the hydrogen bonding probability rises from 0 in bulk water to a maximum of 0.3 at a Pt/midplane distance

Table 2. Calculated and experimental logP values for complexes **1**, **2** and **3**.

	logP			
	MD simulation-based		Structure-based	experimental
Complex	bilayer/water	hydrocarbon/polar region	*n*-octanol/water	
1	–1.788	–2.159	–2.826	–2.19[36]
2	3.083	3.200	1.710	-
3	2.287	2.404	2.777	-

between 8 and 14 Å, where it overlaps with the minimum of the free energy profile. Further decrease in the distance disfavors hydrogen bond formation, also coinciding with an increase in the free energy.

Equilibrium simulations of five Pt-complex molecules in the hydrated DMPC bilayer were also performed to investigate the possible self-aggregation of the complexes and their distribution within the membrane. The local density distributions of the three complexes along the membrane normal, reported in Figure 6b, show good qualitative agreement with the free energy profiles, including both the shift in free energy minimum location and the barrier height at the bilayer midplane for complexes **2** and **3**. This suggests that the distributions in the bilayer are mostly determined by single molecule properties and only to a small extent by concentration-dependent effects. The self-aggregation of platinum complexes was investigated by computing the solvent accessible surface area (SASA), as reported in the Supporting Information. A higher tendency to aggregate was found for complex **3** compared to complex **2**; on the contrary, complex **1**, which resides exclusively in the polar region, has practically no tendency to self-aggregate.

On the basis of the overall results obtained from the MD simulation, the distribution of the three complexes can be represented by the snapshots shown in Figure 7.

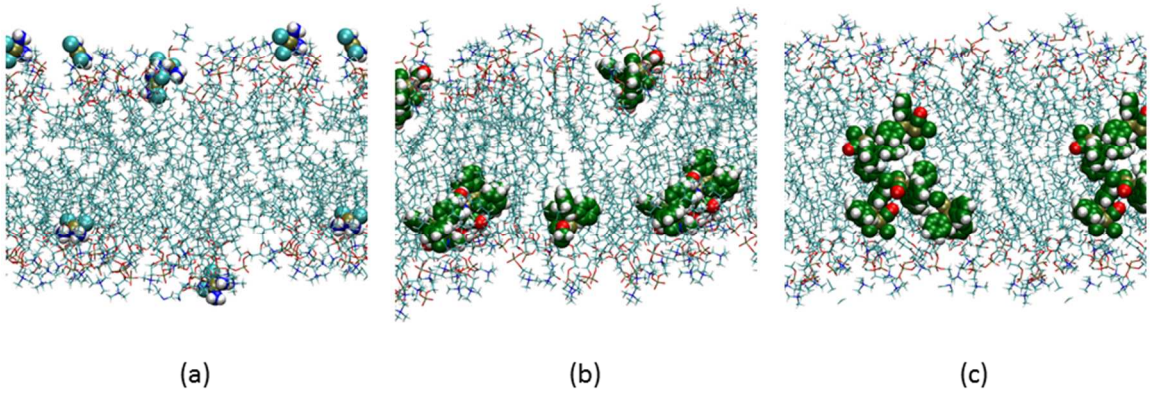

Figure 7. MD simulation snapshots showing a representative distribution of (a) complex **1**, (b) complex **2**, and (c) complex **3** with respect to the DMPC bilayer.

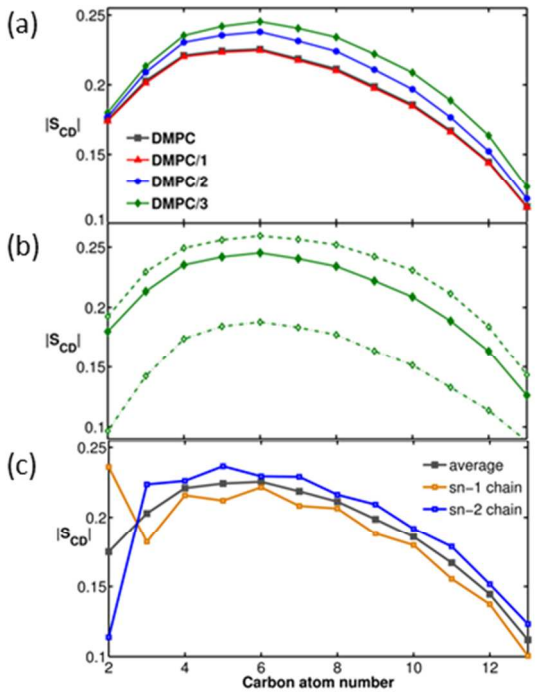

Figure 8. (a) Segmental order parameters of DMPC acyl chains determined from MD calculations for the four samples. The values are averaged over the *sn*-1 and *sn*-2 chains. (b) Average order parameter values for **DMPC/3** (◆) with the trends for the DMPC molecules farthest (dashed curve) and nearest (dot-dashed curve) from complex **3**. (c) Calculated order parameters for the sn-1 and sn-2 chains in **DMPC** and average values.

Equilibrium simulations were also used to calculate average local order parameters for the different methylene groups of the DMPC acyl chains. These were calculated using the following equation:

$$S_{CD_i} = \frac{3}{2}\langle cos^2\theta \rangle - \frac{1}{2} \qquad (3)$$

where θ is the angle between the C_i—D bond vector and the bilayer normal and angular brackets denote averaging over the lipid molecules in the system and over the MD trajectories. The calculated order parameters for the four samples, averaged over the two inequivalent chains of DMPC, are shown in Figure 8a. The trends are characterized by an initial rise in S_{CD} values for the first two methylene groups, followed by an almost constant value of S_{CD} and then a continuous decrease towards the end of the chains. It must be noted that, differently from the experimental values shown in Figure 4 which, as stated before, correspond to the *sn*-1 chain only, the calculated ones are averages over the two chains and hence the initial trend is greatly affected by the low S_{CD} values of the two inequivalent C-D bonds of the first *sn*-2 methylene group. The calculated S_{CD} values for the two different acyl chains are shown in Figure 8c in the case of **DMPC**. As can be observed from Figure 8a, no changes are predicted upon addition of complex **1** to the DMPC bilayers, whereas higher order parameters are calculated for all carbon positions in the case of **DMPC/2** and **DMPC/3**, the latter sample having the higher order.

Discussion

The results of NMR experiments and MD calculations indicated that the three complexes interact in a quite different manner

with the DMPC bilayer. Cisplatin (complex **1**), with a measured logP value of -2.19,[36] is expected not to enter into the hydrophobic region easily, although cisplatin has always been considered to cross membranes also through passive diffusion.[4] The difficulty for cisplatin to enter into the bilayer was here clearly indicated by the free energy values determined in MD calculations. Indeed, the free energy was quite low in the head group region, but rapidly increased becoming too high after the first 5-6 methylene groups of the acyl chains to render the presence of cisplatin in the interior of the bilayer probable (Figures 6a and 7a). All the NMR experiments on **DMPC/1** concurred to indicate that cisplatin accumulates on the bilayer surface. In fact, addition of cisplatin caused a higher ^{31}P chemical shift anisotropy value, at least at the lower temperatures, with respect to **DMPC** (see Table 1). This effect could be due to lower mobility and/or a change in conformation of the head group, as reported for charged species,[37-39] which could here form following cisplatin hydration.[40] The modifications induced by cisplatin on the phospholipid head group, although not predicted from the MD calculations, would have consequences on the whole phospholipid molecule conformation and hence on membrane structure. Electron paramagnetic resonance studies have shown that the binding of cisplatin to the polar head group causes an increase in chain order down to the deeper regions of human erythrocyte membrane.[40] This is exactly what was here observed from ^{2}H NMR spectra of **DMPC/1**, where the local order parameters significantly increased for all methylene and methyl groups of the acyl chains (Figure 4), with a consequent increase in bilayer thickness and a decrease in area per lipid molecule (see Table S3 in the Supporting Information). This, in turn, determined a reduction in membrane elasticity, with an increase of the bilayer bending elastic modulus, which approximately varies as the square of its thickness, by approximately 20%.

Differently from cisplatin, complexes 2 and 3, having positive logP values (Table 2), should preferentially be located within the membrane hydrophobic core, and, on the basis of their permeability values, which are three orders of magnitude larger than that of cisplatin, are expected to be more prone to enter cells by passive diffusion. Moreover, MD calculations indicated that complex **2** has a significantly higher free energy in water and in the polar head group region rather than in the bilayer interior, and that it is located in the hydrophobic region but in the vicinity of the bilayer surface since its di(hydroxyethyl) amine substituent has the ability to form hydrogen bonds with the carbonyl and phosphate groups (Figures 6c and 7b).

In agreement with these findings, the ^{31}P NMR spectra did not show conformational or motional changes for the phosphate group (Figure 2 and Table 1), thus excluding relevant interactions between complex **2** and the DMPC head group within the polar region. On the other hand, the slight increase in acyl chain order up to two thirds of the chain, put in evidence by the ^{2}H NMR spectra (Figures 3 and 4), and in agreement with the calculated order parameter values, experimentally confirms that complex **2** preferentially resides in the upper region of the acyl chains, only slightly modifying the bilayer thickness and having a minor effect on the bending elastic modulus, which increases only by ~4%.

A completely different behavior was observed for complex **3**. On the basis of MD calculations it could be inferred that this complex entered well within the hydrophobic interior of the bilayer, residing closer to the bilayer midplane than complex **2**, as depicted in Figure 7c. In fact, the barrier for diffusion within the bilayer is much lower than that calculated for cisplatin (see Figure 6a). The ^{31}P, ^{2}H, as well as ^{13}C NMR spectra of **DMPC/3** gave strong evidence of lateral phase separation due to the insertion of the complex into the bilayer, with the formation of two distinct phospholipidic environments above T_c, one similar to a liquid-ordered (L_o) phase, the other being an L_α domain. The term liquid-ordered was coined to define domains formed by lipids with ordered and extended acyl chains, but still exhibiting the high mobility characteristic of a liquid.[41] The L_o phase has been reported to coexist with the L_α phase in saturated phospholipid systems containing cholesterol, the latter accumulating in the L_o phase.[21] In **DMPC/3** the L_o domains were indeed characterized by an all-trans chain conformation, as indicated by the high quadrupolar splittings in the ^{2}H NMR spectra (Figure 3) and the high chemical shift value of the chain methylene carbons in the ^{13}C spectra (Figure 5). The lack of changes in overall width of the ^{2}H spectra with the temperature suggested that the chain order did not change, the higher resolution observed at higher temperature probably arising from an increase in overall molecular rotation and wobbling motions. As far as the phospholipid head group is concerned, the ^{31}P spectra showed two components: one axially symmetric, as expected for L_α phases, and the other one slightly asymmetric. The former was characterized by a $\Delta\sigma$ value of 33 ppm at high temperature, quite smaller than that observed for the other samples; such a low $\Delta\sigma$ value, which was not paralleled by a reduction in ^{2}H quadrupolar splittings of the chain methylene groups, is not ascribable to a motional process, and can be justified only assuming a small change in head group conformation. The asymmetric component in the ^{31}P spectra is ascribable to the L_o domains, and, again, is probably due to a head group conformation which differs from that in the other samples. The presence of two distinct ^{2}H subspectra for **DMPC/3** allowed the lower bound for the L_o and L_α domain size in the bilayer to be roughly estimated as described in the Supporting Information. With the simplifying assumption of a similar size for the two domains, the minimum domain size at 40 °C was estimated to be ~90 nm.

Although the NMR results gave unambiguous evidence of the lateral phase separation, they gave no clues on where complex **3** resides. This information can be retrieved from the segmental order parameters for the methylene and methyl C-D bonds of the DMPC alkyl chains determined by MD calculations, which clearly showed that complex **3** is preferentially located in the L_α phase. In fact, although in the case of **DMPC/3** higher average chain ordering was predicted with respect to DMPC alone, the order parameter profiles clearly indicated that the DMPC molecules in the proximity of the complex were less ordered, whereas those located farther away were significantly more ordered (Figure 8b). In agreement with the NMR findings, this suggests that complex **3** divides the DMPC molecules into two populations: less ordered in the direct vicinity and more ordered farther away. This effect is probably due to the fact that complex **3** is, on average, located close to the membrane midplane (Figures 6b and 7c) and has a strong tendency to self-aggregate inside the bilayer, as suggested by the calculated SASA (Figure S4 in the Supporting Information).

Experimental

Materials

The synthetic procedures reported in the literature were used to prepare cisplatin[42] and complexes **2** and **3**.[6,8] DMPC and alkyl chain perdeuterated DMPC-d_{54} were purchased from Avanti

Polar Lipids. Deuterium-depleted water (≤ 1 ppm D_2O) was purchased from Aldrich.

NMR sample preparation

All samples were prepared using a mixture of DMPC and DMPC-d_{54} in a weight ratio 70:30, except for the DMPC sample used for ^{2}H NMR experiments which was prepared using solely DMPC-d_{54}. Thus, the samples were **DMPC** (hydrated DMPC-d_{54} or DMPC/DMPC-d_{54} mixture), and **DMPC/1**, **DMPC/2**, **DMPC/3** (hydrated DMPC/DMPC-d_{54} mixture added with complexes **1**, **2** or **3**, respectively). In all cases the following procedure was used. Either the phospholipid alone or mixed with the Pt complex in a 9:1 DMPC to complex molar ratio was dissolved in a small quantity of chloroform, which was subsequently removed by air drying followed by vacuum drying overnight. The dried powder was added with deuterium depleted water obtaining MLV samples with 32 wt% of water which were subjected to 5 freeze-thawing cycles.[43,44] Finally the samples were inserted in 4 mm diameter zirconia rotors for NMR experiments. The DMPC MLVs obtained should have a phase transition from a gel phase $P_{\beta'}$ to a liquid crystalline phase L_α at a temperature of 23°C, which for DMPC-d_{54} is reduced to 19.5 °C because of deuteration; for systems containing 70:30 DMPC/DMPC-d_{54} the transition temperature is expected between 20 °C and 23.6 ± 1.5 °C.[20]

NMR experiments

NMR spectra were acquired on a Bruker AMX300WB spectrometer working at 300.13 MHz on proton, equipped with a cross polarization magic angle spinning (CP-MAS) 4mm probe, using 4 mm zirconia rotors with Kel-F caps. ^{31}P, ^{2}H and ^{13}C NMR spectra were recorded from 20 to 40 °C at 5 °C intervals. The temperature was controlled using a BT1000 variable temperature unit; the temperature was stable within ± 1 °C.

^{31}P NMR spectra were acquired at 121.49 MHz with direct excitation and high-power ^{1}H decoupling during acquisition, with a 90° pulse duration of 2.5 μs, a recycle delay of 5 s and accumulating 200 scans. The spectra were recorded on static samples and analysed using the WSOLIDS1 software (version 1.20.21, Copyright (C) 1994, 2012 Klaus Eichele). The chemical shifts were referenced to an external 85 wt% H_3PO_4 sample.

^{2}H NMR spectra were acquired at 46.07 MHz using a quadrupolar echo pulse sequence with a 90° pulse duration of 6.5 μs, an echo time of 50 μs, a recycle delay of 2 s and accumulating 8000 scans. The spectra were recorded on static samples; the resulting powder spectra were de-Paked using the NMR Depaker 1.0rc1 software (Copyright (C) 2009 Sébastien Buchoux).[22]

^{13}C cross polarization with magic angle spinning (CP-MAS) NMR spectra were acquired at 75.47 MHz, with a 90° pulse duration of 4.5 μs, a cross polarization contact pulse of 5 ms, a recycle delay of 3 s and accumulating 200 scans. The spinning rate was 2 kHz, thus avoiding centrifugal effects and sample heating.

MD simulations

Free energy calculations. Free energy profiles were obtained using the umbrella sampling method. Each simulation model contained one Pt(II) complex molecule and 64 DMPC molecules arranged in a bilayer in the *xy* plane, solvated with 2847 water molecules. DMPC molecules were modeled using CHARMM36[45] force field parameters and the TIP3P model was used for water. Bonded and Lennard-Jones parameters for the Pt complexes were taken from the general purpose CHARMm force field.[46] The partial charges for the Pt complexes were obtained from DFT/B3LYP calculations in Gaussian[47] *via* Merz-Kollman ESP fitting, using the LANL2DZ basis set with LANL2 pseudopotentials[48] for Pt atoms and the 6-31G* basis for the remaining atomic species. The simulations were carried out using NAMD[49] in NPT ensemble. The temperature was kept at 310 K using a Langevin thermostat and the pressure was kept at 1 bar using the Langevin piston algorithm.[50] Van der Waals interactions were represented by the Lennard-Jones potential with a smooth cutoff with a switching radius of 10 Å and a cutoff radius of 12 Å. Particle Mesh Ewald with a real-space cutoff of 10 Å was used to account for long-range electrostatic interactions.[51] The velocity Verlet algorithm was used to integrate the equations of motion with the time step set to 2 fs. The reaction coordinate z for umbrella sampling calculations was defined as the z-component of the distance vector from the bilayer center of mass to the Pt atom. The transfer pathway, defined as the interval $0 < z < 28$ Å (where 0 and 28 Å correspond to the bilayer mid-plane and the bulk water region, respectively), was divided into 15 equally sized windows. To hold the platinum compounds around a set of the reference distance values, a harmonic biasing potential was applied with the spring constant of 4.0 kJ mol^{-1}Å^{-2} for complex **1**, 2.0 kJ mol^{-1}Å^{-2} for complex **2** and 1.2 kJ mol^{-1}Å^{-2} for complex **3**. For each of these windows, 400 ns of trajectory was generated, and the data were later post-processed by the Weighted Histogram Analysis Method[52] to remove the effect of artificial potentials and recover the unbiased free energy profiles.

The probability of hydrogen bond formation as a function of z was computed from the umbrella sampling simulations as the fraction of trajectory frames that correspond to an existing h-bond when the platinum compound is located within the interval (z-δz, z+δz). Contributions from individual frames were reweighted by a factor $\exp[(U_i(z) - F_i)/k_BT]$, where F_i denotes the free energy offset for the i-th window derived from the WHAM procedure, and $U_i(z)$ is the energy of the harmonic restraint in the i-th window.

Equilibrium MD simulations. Equilibrium simulations were carried out on systems comprising 64 DMPC molecules arranged in a bilayer, with 2546 explicit water molecules, added in order to fill the rectangular box (49.1×42.5×74.2 Å), K^+/Cl^- ions to provide physiological ionic concentration (0.154 M), and 5 Pt complex molecules. The force field parameters applied were the same as above. The simulations were conducted with the Gromacs suite[53] for a total time of 1 μs with a 2 fs time step, in periodic boundary conditions and in the NPT ensemble with a reference temperature of 315 K and a reference pressure of 1 bar. Van der Waals and short-range Coulomb interactions cutoff was set to 12 Å and 10 Å, respectively, and the PME scheme was employed to compute long-range electrostatics.

Conclusions

In the present study, the combined use of NMR experiments and MD calculations proved to be fundamental in obtaining a consistent picture of the phenomena that take place when the

different complexes investigated encounter the DMPC bilayer. The differences observed among the three Pt(II) complexes investigated could, partly, be responsible for their different antitumoral efficacy which was found to follow the order complex **1** ~ complex **2** >> complex **3**.

Experimental and computational evidence indicated that cisplatin preferentially interacts with the bilayer surface, showing a low tendency to enter within the hydrophobic core of the bilayer, thus excluding a relevant contribution of passive diffusion in cellular uptake and excretion, at least in a simple system as the one here considered. On the contrary, for complex **2**, both NMR and MD results suggested that passive diffusion may be important. This feature may represent an advantage for this potential drug since its action on cells cannot be impaired by common drug resistance mechanisms, such as down-regulating the expression of transmembrane transporters and channels.[54] On the other hand, cisplatin has a stronger effect on bilayer thickness and elasticity which affects membrane-mediated mechanical response in cells.

The case of the complex **3** is quite peculiar. Both NMR and MD findings point to the formation of laterally separated complex-rich and phospholipid-rich domains characterized by significantly different mobility. How this may affect the membrane structure and functioning is not clear yet, although membrane structure, in addition to membrane chemistry, certainly determine many cell properties. To the best of our knowledge, this is the first time large scale lateral phase separation with formation of phospholipid rich liquid ordered domains is reported. Further investigations to this regard are necessary.

Acknowledgements

TASK and Cyfronet computational centers are thanked for having granted CPU time.

Notes and references

[a] Department of Physical Chemistry, Gdansk University of Technology, ul. Narutowicza 11/12, 80-233 Gdansk, Poland.
[b] Department of Chemistry and Industrial Chemistry, University of Pisa, via Risorgimento 35, 56126 Pisa, Italy.
[c] Department of Pharmaceutical Technology and Biochemistry, Gdansk University of Technology, ul. Narutowicza 11/12, 80-233 Gdansk, Poland.
[d] Institute of the Chemistry of Organometallic Compounds, CNR, via G. Moruzzi 1, 56124 Pisa, Italy.

† Corresponding authors: Claudia Forte: claudia.forte@pi.iccom.cnr.it; Jacek Czub: jacczub@pg.gda.pl.
‡ Present address: Dipartimento DICATECh, Politecnico di Bari, Via Edoardo Orabona 4, 70125 Bari, Italy.

Electronic Supplementary Information (ESI) available: Antitumoral properties of Pt(II) complexes; ^{31}P NMR spectrum of DMPC/3 at 40 °C; analysis of ^{2}H NMR spectra; convergence of the free energy profiles; calculation of partition and permeability coefficients; calculation of solvent accessible surface area; calculation of phospholipid domain size. See DOI: 10.1039/b000000x/

1 L. Kelland, *Nat. Rev. Cancer* 2007, **7**, 573.
2 B. W. Harper, A. M. Krause-Heuer, M. P. Grant, M. Manohar, K. B. Garbutcheon-Singh and J. R. Aldrich-Wright, *Chem. Eur. J.* 2010, **16**, 7064.
3 X. Wang and Z. Guo, *Chem. Soc. Rev.* 2013, **42**, 202.
4 D. P. Gately and S. B. Howell, *Br. J. Cancer* 1993, **67**, 1171.
5 F. Arnesano, M. Losacco and G. Natile, *Eur. J. Inorg. Chem.* 2013, 2701.
6 L. Dalla Via, A. N. García-Argáez, A. Adami, S. Grancara, P. Martinis, A. Toninello, D. Belli Dell'Amico, L. Labella and S. Samaritani, *Bioorg. Med. Chem*. 2013, **21**, 6965.
7 F. J. Ramos-Lima, A. G. Quiroga, B. García-Serrelde, F. Blanco, A. Carnero and C. Navarro-Ranninger, *J. Med. Chem.* 2007, **50**, 2194.
8 D. Belli Dell'Amico, C. Broglia, L. Labella, F. Marchetti, D. Mendola and S. Samaritani, *Inorg. Chim. Acta* 2013, **395**, 181.
9 V. Censi, Master's Thesis in Chemistry, University of Pisa, 2013, http://etd.adm.unipi.it/.
10 M. J. Janiak, D. M. Small and G. G. Shipley, *J. Biol. Chem.* 1979, **254**, 6068.
11 M. F. Brown, S. Lope-Piedrafita, G. V. Martinez and H. I. Petrache, in *Modern Magnetic Resonance*, ed. G. A. Webb, Springer, Heidelberg, 2006, pp 245-256.
12 J. Schiller, M. Muller, B. Fuchs, K. Arnold and D. Huster, *Curr. Anal. Chem.* 2007, **3**, 283.
13 S. E. Feller, *Curr. Opin. Colloid Interface Sci.* 2000, **5**, 217.
14 M. Orsi and J. W. Essex, *Soft Matter* 2010, **6**, 3797.
15 D. Bemporad, C. Luttmann and J. W. Essex, *Biochim. Biophys. Acta Biomembranes* 2005, **1718**, 1.
16 E. J. Dufourc, C. Mayer, J. Stohrer, G. Althoff and G. Kothe, *Biophys. J.* 1992, **61**, 42.
17 J. Seelig, *Biochim. Biophys. Acta Rev. Biomembranes* 1978, **515**, 105.
18 K. Belohorcová, J. Qian and J. H. Davis, *Biophys. J.* 2000, **79**, 3201.
19 H. I. Petrache, S. W. Dodd and M. F. Brown, *Biophys. J.* 2000, **79**, 3172.
20 D. Guard-Friar, C. H. Chen and A. S. Engle, *J. Phys. Chem.* 1985, **89**, 1810.
21 S. L. Veatch, I. V. Polozov, K. Gawrisch and S. L. Keller, *Biophys. J.* 2004, **86**, 2910.
22 E. Sternin, M. Bloom and A. MacKay, *J. Magn. Reson.* 1983, **55**, 274.
23 E. Oldfield, M. Meadows, D. Rice and R. Jacobs, *Biochemistry* 1978, **17**, 2727.
24 J. A. Urbina, S. Pekerar, H.-B- Le, J. Patterson, B. Montez and E. Oldfield, *Biochim. Biophys. Acta* 1995, **1238**, 163.
25 F. Aussenac, M. Laguerre, J.-M- Schmitter and E. J. Dufourc, *Langmuir* 2003, **19**, 10468.
26 J.-P. Douliez, A. Léonard and E. J. Dufourc, *J. Phys. Chem.* 1996, **100**, 18450.
27 K. J. Mallikarjunaiah, A. Leftin, J. J. Kinnun, M. J. Justice, A. L. Rogozea, H. I. Petrache and M. F. Brown, *Biophys. J.* 2011, **100**, 98.
28 J. H. Davis, *Biophys. Biochim. Acta* 1983, **737**, 117.
29 K. A. Henzler-Wildman, G. V. Martinez, M. F. Brown and A. Ramamoorthy, *Biochemistry* 2004, **43**, 8459.
30 M. R. R. De Planque, D. V. Greathouse, R. E. Koeppe II, H. Schafer, D. Marsh and J. A. Killian, *Biochemistry* 1998, **37**, 9333.
31 K. Nomura, M. Lintuluoto and K. Morigaki, *J. Phys. Chem. B* 2011, **115**, 14991.
32 W. L. Earl and D. L. VanderHart, *Macromolecules* 1979, **12**, 762.
33 I. Vorobyov, W. F. D. Bennett, D. P. Tieleman, T. W. Allen and S. Noskov, *J. Chem. Theory Comput.* 2012, **8**, 618.
34 J. P. M. Jämbeck and A. P. Lyubartsev, *Phys. Chem. Chem. Phys.* 2013, **15**, 4677.
35 Molinspiration, www.molinspiration.com/cgi-bin/properties.
36 J. P. Souchard, T. T. B. Ha, S. Cros and N. P. Johnson, *J. Med. Chem.* 1991, **34**, 863.
37 P. G. Scherer and J. Seelig, *Biochemistry* 1989, **28**, 7720.
38 J. S. Santos, D.-K. Lee and A. Ramamoorthy, *Magn. Reson. Chem.* 2004, **42**, 105.
39 M. F. Brown and J. Seelig, *Nature* 1977, **269**, 721.
40 K. Wang, J. Lu and R. Li., *Coord. Chem. Rev.* 1996, **151**, 53.
41 J. H. Ipsen, G. Karlström, O. G. Mouritsen, H. Wennerström and M. J. Zuckermann, *Biochim. Biophys. Acta* 1987, **905**, 162.
42 S. C. Dhara, *Ind. J. Chem.* 1970, **8**, 193.
43 L. D. Mayer, M. J. Hope, P. R. Cullis and A. S. Janoff, *Biochim. Biophys. Acta Biomembranes* 1985, **817**, 193.
44 M. J. Hope, M. B. Bally, L. D. Mayer, A. S. Janoff and P. R. Cullis, *Chem. Phys. Lipids* 1986, **40**, 89.
45 B. Best, X. Zhu, J. Shim, P. Lopes, J. Mittal, M. Feig and A. D. MacKerell, Jr., *J. Chem. Theory Comput.* 2012, **8**, 3257.
46 F. A. Momany and R. Rone, *J. Comput. Chem.* 1992, **13**, 888.

47 M. J. Frisch, et al. Gaussian 09, Revision B.1; Gaussian Inc.: Wallingford, CT, 2009.
48 P. J. Hay and W. R. Wadt, *J. Chem. Phys.* 1985, **82**, 270.
49 J. C. Phillips, R. Braun, W. Wang, J. Gumbart, E. Tajkhorshid, E. Villa, C. Chipot, R. D. Skeel, L. Kalé and K. Schulten, *J. Comput. Chem.* 2005, **26**, 1781.
50 S. E. Feller, Y. Zhang, R. W. Pastor and R. B. Brooks, *J. Chem. Phys.* 1995, **103**, 4613.
51 T. Darden, D. York and L. Pedersen, *J. Chem. Phys.* 1993, **98**, 10089.
52 S. Kumar, D. Bouzida, R. H. Swendsen, P. A. Kollman and J. M. Rosenberg, *J. Comput. Chem.* 1992, **13**, 1011.
53 B. Hess, C. Kutzner, D. van der Spoel and E. Lindahl, *J. Chem. Theory Comput.* 2008, **4**, 435.
54 D. W. Shen, L. M. Pouliot, M. D. Hall and M. M. Gottesman, *Pharmacol. Rev.* 2012, **64**, 706.